

# Characterization of the expected seismic damage for a critical infrastructure: the case of the oil pipeline in Friuli Venezia Giulia (NE Italy)

Alberto Tamaro<sup>1,2</sup>  · Stefano Grimaz<sup>2</sup> · Marco Santulin<sup>3</sup> · Dario Slejko<sup>1</sup>

Received: 24 September 2016 / Accepted: 21 October 2017 / Published online: 27 October 2017  
© Springer Science+Business Media B.V. 2017

**Abstract** Seismic codes using the performance-based approach for seismic design of critical and important structures generally refer to seismic hazard which takes into account a lower exceedance probability than that used for ordinary buildings. In the present study, the seismic hazard for an oil pipeline, located in the Friuli Venezia Giulia region (NE Italy), has been calculated in terms of PGA and PGV with a 2475-year return period, and compared with estimates calculated with the standard 475-year return period used for ordinary buildings. The results, referring to three soil types (rock, stiff soil, and soft soil), have been combined through GIS technology in a single map (soil seismic hazard map) on the basis of the local lithological characterization. The major earthquakes considered in the study have been associated with the linear sources found in the database of Italian seismic sources, considering the characteristic earthquake model. The regional seismogenic zonation has been added to the linear sources in order to consider minor seismicity as described by the Gutenberg–Richter model. Quaternary faults in the broader Trieste area, long enough to justify, at least, a characteristic magnitude of 6, have been added in the source model to take into account unlikely but possible unknown sources. The Transalpine Oil Pipeline, which connects Trieste (Italy) to Ingolstadt (Germany), is the crude-oil distribution system considered in the present study. It consists of a storage tank, compressor stations, and buried pipeline. For the characterization of the expected damage to the infrastructure in case of an earthquake, we have used underground pipeline seismic vulnerability curves that relate a performance indicator, such as the reparation rate (number of ruptures per kilometre), with a representative ground motion parameter (e.g., PGA or PGV). In this study, we have considered as performance indicator the consequences of a rupture in the pipeline caused by a seismic event.

---

✉ Alberto Tamaro  
atamaro@inogs.it

<sup>1</sup> Istituto Nazionale di Oceanografia e di Geofisica Sperimentale – OGS, Trieste, Italy

<sup>2</sup> Dipartimento Politecnico di Ingegneria e Architettura, Università degli Studi di Udine, Udine, Italy

<sup>3</sup> Istituto Nazionale di Geofisica e Vulcanologia, Sezione di Milano, Italy c/o OGS, Trieste, Italy

**Keywords** Soil seismic hazard · Critical infrastructure · Oil system vulnerability · Fragility curve · Loss containments · GIS spatial analysis · Friuli · NE Italy

## 1 Introduction

Earthquakes not only cause the collapse of buildings, bridges, etc., with loss of human lives, but the seismic damage can also undermine the local economic and social structure especially in the case of critical and strategic infrastructures and might initiate severe impacts to the environment (Clemente 2013). Earthquakes, in fact, can cause emissions of dangerous matter deriving from significant damage to storage and energy transportation systems, such as oil and gas pipelines. The severity of such incidents can be further amplified by the possible concurrent failure of mitigation systems designed to contain the earthquake consequences, such as the breaking of fire water pipes (Grimaz 2014). These kinds of events have been named Na-Tech (Natural Hazards Triggering Technological Disasters) incidents (Campedel et al. 2008; Krausmann et al. 2011) to indicate the double origin of the events: natural and technological.

The most dramatic example of a Na-Tech incident occurred during the  $M_w = 9.0$  Tohoku earthquake on March 11, 2011, off the east coast of Japan. Although the damage caused by the ground shaking of this powerful earthquake can be considered limited, the earthquake caused a tsunami that after a few minutes reached the Japanese coast. Waves about 14 m high crashed into the Fukushima Daiichi nuclear power plant, passing the barriers (about 6 m high) and invading the premises of the plant. Because the emergency power generators were phased out and stopped the fuel-cooling process, an uncontrolled overheating melted the fuel rods, causing the explosion of three reactors. This incident resulted in an environmental disaster involving radioactive pollution (Genn 2014). Another example is the  $M_w = 7.4$  earthquake of Koaceli, Turkey, in 1999, which caused a fire and subsequent collapse of a refinery tank in Izmit with terrible consequences in terms of atmospheric pollution (Girgin 2011). A further example is what happened during the  $M_w = 6.7$  Northridge, California, earthquake of January 17, 1994: Lindell and Perry (1997) reported many ruptures at the Arco Four Corners pipeline and estimated that more than 8700 m<sup>3</sup> of crude oil leaked near the city of Santa Clarita and, travelling through a drainage channel, flowed into the Santa Clara River. Although all the petroleum pipeline pumping stations shut down within about 1 min of the earthquake detection, reducing the pipeline pressure, the spills could not be prevented. The release of oil and the cleanup operations impacted about 40 ha of woody and herbaceous vegetation and about 60 ha of river sediments (<http://enatech.jrc.ec.europa.eu/Natech/44>). It is also important to remember the  $M_L = 7.2$  earthquake of Yushu, China, in April 2010, which caused much damage both to road infrastructure and to electricity transmission systems; there was also serious damage and breaks in underground water conduits caused by superficial faulting phenomena and by *debris flows*.

Recent studies have explored seismic hazard evaluation for critical infrastructures (e.g., Grimaz and Slejko 2014) and, in particular, the Italian situation; other studies have examined the potential of Italian earthquakes for triggering major accidents (Grimaz 2014).

Regarding planned infrastructures, it is important to evaluate the potential effects of natural disasters in order to identify the best sites for construction. In the case of existing infrastructures, it is best to estimate the damage that would occur in the case of an earthquake and to identify the components needing specific countermeasures.

This study is aimed at analysing the seismic hazard of a territory crossed by a linear infrastructure, such as an oil pipeline, and at assessing the expected damage caused by a seismic event, in order to plan mitigation actions according to established priorities. More specifically, the aim of the present study is to define decision-making support by developing a geo-database (Bogliolo 2012) destined to collect and manage geospatial data. Such data are necessary to develop preliminary actions for seismic risk mitigation through the identification of potentially dangerous areas to place a crude oil distribution system, made of an underground oil pipeline, pumping stations, and storage tanks.

The main problem regarding the analysis of the seismic risk for an underground pipeline is the choice of an adequate parameter characterizing the strong ground motion. In the literature many different parameters have been used to represent the seismic shaking in the fragility function, based on empiric data from past earthquakes.

Initially, Eguchi (1983), O'Rourke et al. (1991) and O'Rourke and Ayala (1993) applied the Mercalli Modified macroseismic intensity as damage indicator for underground pipelines. The installation of seismic stations, and the subsequent availability of accelerometer records, allowed the estimation of physical parameters such as peak ground acceleration (PGA) and peak ground velocity (PGV), better correlated to the damage suffered by underground pipeline during an earthquake.

PGA has been widely used as damage indicator for underground structures (see, e.g., Katayama et al. 1975; Isoyama and Katayama 1982; Hamada 1991; O'Rourke et al. 1998; Isoyama et al. 2000). In particular, Katayama et al. (1975) used the data of 6 strong earthquakes (Kanto 1923  $M_w = 7.9$ , Fukui 1948  $M_w = 6.8$ , Niigata 1964  $M_w = 7.6$ , Tokachi-Oki 1968  $M_w = 8.3$ , San Fernando 1971  $M_w = 6.7$ , Managua 1972  $M_w = 6.3$ ) to derive empirical scaling laws between PGA and repair rate (number of repairs for a given pipeline length).

The principal damage suffered by an underground pipeline during an earthquake is represented by its rupture caused by a permanent ground deformation (PGD). As a direct measurement of the ground deformation is rarely available, scaling laws have been developed to correlate other parameters to ground deformation. Although it was empirically demonstrated (O'Rourke and Ayala 1993; Isoyama et al. 2000; ALA 2001) that PGV is better correlated to underground pipeline damage than PGA, the scarce availability before the twenty-first century of actual PGV recordings (not obtained from PGA by mathematical integration) and the worldwide use of PGA ground motion prediction equations (GMPEs) forced the use of PGA as shaking parameter in the fragility curves.

## 2 Seismic risk for critical facilities

As it is impossible to reduce seismic hazard, seismic risk mitigation consists of limiting earthquake consequences by taking steps to reduce vulnerability and exposure, and appropriately planning land use, in particular when environmental pollution is a concern. To accomplish this, GIS technology offers a fundamental computer support to manage and represent spatial data deriving from the probabilistic analyses of seismic hazard and risk.

Seismic risk assessment combines three main components: seismic hazard, vulnerability, and exposed value. In the present case, we do not consider the exposed value and calculate only the expected damage for the oil pipeline system, instead of the expected economic loss.

The starting point in the methodology aiming at an estimation of the expected damage to an underground infrastructure is represented by the analysis of the seismic hazard which, for a distribution system of crude oil, should include, based on the experience collected through the years (O'Rourke and Liu 1999), both the ground motion along the infrastructure route, which can induce also landslides and liquefaction, and the soil permanent deformation causing superficial faulting (ground failure) with related ruptures of the infrastructure.

Even if the expected damage to the underground pipeline is 3 or 4 times lower than that caused by permanent ground deformation (O'Rourke et al. 1991), the present study focuses, in particular, on the seismic ground motion along the infrastructure, i.e., the transient ground deformation. This is motivated by the fact that some earthquakes have shown that the largest damage to infrastructures was mainly caused by seismic waves propagation, strongly amplified by local soil conditions. This is the case of the 1985 Michoacan earthquake which caused remarkable damage to underground pipelines in Mexico City.

The first calculation, seismic hazard, has been developed according to the probabilistic approach originally proposed by Cornell (1968). This method is based on the characterisation of the seismic sources and consequentially determines the shaking expected at the site in terms of PGA and PGV, through the application of suitable GMPEs.

The second calculation involves the physical vulnerability of the oil pipeline infrastructure (anchored atmospheric steel tank, oil pipeline, pumping station), expressed in terms of predisposition to direct physical damage in the case of an earthquake. This damage is evaluated through fragility curves, which are cumulative log-normal functions that give the probability the pipeline will reach, or exceed, different damage states, given the strength of the ground shaking to which the considered element is subjected. In most of the studies in literature, the seismic vulnerability of the underground structures has been described by curves showing a performance indicator, such as the reparation value (number of breakings, and therefore reparations, per kilometre), depending on the ground shaking (e.g., Mercalli Modified intensity, PGA, PGV). These curves were, generally, calculated on the basis of empirical (observational) data without considering the possible contaminative release of dangerous substances in the surrounding environment, caused by the damage suffered by the underground pipeline. Moreover, most of the fragility functions have been modelled on segmented conducts, as in the case of water or waste pipelines, instead of continuous underground pipelines, as oil pipelines are.

To take the above aspects into consideration, the Lanzano et al. (2013a, b) methodology, that considers the consequences (e.g., the environmental pollution) of the damage suffered by a continuous buried pipeline under earthquake loading, has been applied in the present study. This methodology considers different states of risk and quantifies the amounts of oil that would leak into the environment. Moreover, the Fabbrocino et al. (2005) methodology has been applied in the case of the anchored atmospheric steel tank, and, finally, the HAZUS methodology (NIBS 2004), that considers four damage states, has been used for the pumping station.

The results of a seismic hazard analysis have been combined with the fragility function and the mean probability in 50 years for different levels of oil loss into the external environment has been computed for each element of the system.

The described methodology has been applied for the seismic risk evaluation of the Transalpine (TAL) Pipeline, which links Trieste (Italy) to Ingolstadt (Germany). TAL is part of a pipeline network running throughout Europe (Fig. 1a). The infrastructure begins at the marine terminal in the Trieste Gulf (Fig. 1b), where crude oil (on average 35 million

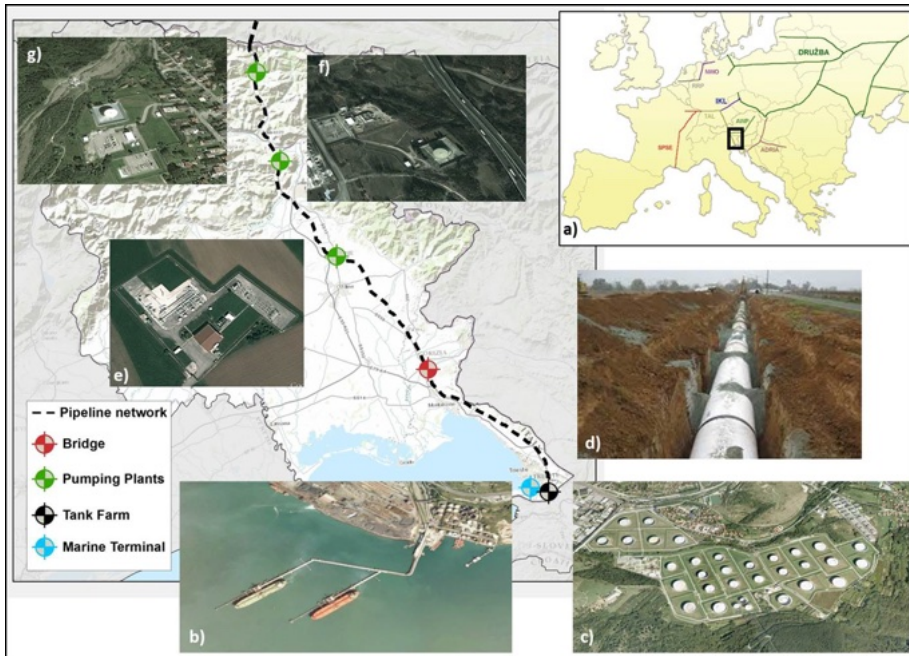


**Fig. 1** The TAL pipeline: the crude oil pipeline network in Europe is shown in (a), and the black box identifies the TAL pipeline area considered in the present study. The TAL infrastructure begins at the marine terminal in the Trieste Gulf (b), where crude oil (on average 35 million tonnes per year) is discharged and transferred to the Dolina tank farm (c). From there, the primarily underground pipeline (d; the image is approximate and does not represent the actual route of the TAL pipeline) crosses the entire Friuli Venezia Giulia territory (see the region in the background). Along the route of the TAL pipeline, there are three pumping stations (e–g)

tonnes per year) is discharged from ships and transferred to the Dolina Tank Farm (Fig. 1c) through four underground pipelines. From there, the underground pipeline goes across the entire territory of the Friuli Venezia Giulia region in Italy and, after crossing the Alps, it proceeds through Austria to reach Ingolstadt in Germany. There, it divides into two, ending to the west near Karlsruhe and to the east at Neustadt, both in Germany, for a total of 753 km. The seismic risk analysis presented here focuses on the section located in Friuli Venezia Giulia, consisting of the marine landing facility (Fig. 1b), the storage station (Fig. 1c), the three pumping stations (Fig. 1e–g), and the pipeline, which is mostly underground (Fig. 1d).

### 3 Seismic hazard along the TAL route

The probabilistic approach originally proposed by Cornell (1968) has been applied for the study of seismic hazard, using the Crisis 2015 software (Ordaz et al. 2015). The Cornell (1968) approach is based on two hypotheses: (1) the earthquake occurrence intervals have an exponential distribution (that is, the events form a Poisson process); (2) magnitude is distributed exponentially according to the Gutenberg–Richter (GR) relation. Furthermore, seismicity is considered to be uniformly distributed inside the seismic sources. The Cornell

(1968) method needs the following input data: seismic source geometry, seismicity model (in terms of average number of earthquakes per magnitude class, and maximum magnitude), and ground motion attenuation model. Uncertainty quantification (McGuire 1977) represents a crucial point in probabilistic seismic hazard analysis (PSHA). In fact, PSHA results are characterized by two kinds of uncertainty: the aleatory variability and the epistemic uncertainty (McGuire and Shedlock 1981; Toro et al. 1997). The aleatory variability is the natural randomness in a process: in PSHA, it is included in computations by introducing the attenuation model standard deviation. The epistemic uncertainty is the scientific uncertainty in the choice of the model for the process, and it is caused by limited data and knowledge: it is accounted for by using different models. The logic tree approach in PSHA (Kulkarni et al. 1984; Coppersmith and Youngs 1986) was introduced to quantify the epistemic uncertainties. It consists of a series of nodes at which models are specified (seismogenic zonation, seismicity model, attenuation model, etc.) and branches that represent the different models specified at each node, weighted accordingly. The models considered in the logic tree must be exhaustive (representing all informed scientific community opinions) and mutually exclusive. The sum of the probabilities of all branches connected to a given node must be 1. The overall final result (mean value and standard deviation) is achieved by carefully weighting the individual results derived from different branches (Rebez and Slejko 2004).

The present study has employed a logic tree simpler than that already used for the seismic hazard assessment of Friuli Venezia Giulia (Slejko et al. 2011b). It is composed of two seismogenic zonations [Fig. 2, FRI (Slejko et al. 2008) and DISS (DISS Working Group 2010)], one seismicity model (Slejko et al. 1998), one statistical method for maximum magnitude calculation (Kijko and Graham 1998), and one GMPE (Bindi et al. 2011) for PGA and PGV. Given the importance of the oil pipeline, seismic hazard has been evaluated with a return period ( $T_r$ ) of 2475 years, corresponding to the exceedance probability of 2% in 50 years. Moreover, a  $T_r$  of 475 years, corresponding to the exceedance probability of 10% in 50 years, i.e., the standard reference for ordinary buildings, has been considered as well. Calculations have been done for three soil types: rock, stiff soil, and soft soil, according to the soil map of Friuli Venezia Giulia (Slejko et al. 2011b).

To identify near-field effects (Grimaz 2012; Grimaz and Malisan 2014), the major earthquakes have been associated with the linear sources in the database of the Italian seismic sources [DISS: DISS Working Group (2010)], and for them the characteristic earthquake model has been considered. This model was introduced by Schwartz and Coppersmith (1984) for the seismicity in California, where it is supposed that each fault can only generate earthquakes with a determined ( $\pm 0.5$ ) magnitude, called “characteristic”, according to the geometric dimension of the possible rupture along the fault. In agreement with this model, Wells and Coppersmith (1994) developed scale relations between fault rupture dimensions and magnitude. Lack of data and difficulty in associating earthquakes to faults do not allow seismologists to decide, yet, if this model is valid everywhere, valid only in relation to certain faults, or not valid at all. Going into the details of our work, we have considered the recurrence intervals reported in DISS and have associated an uncertainty of  $\pm 0.3$  to the characteristic earthquake magnitudes, also taken from DISS (Table 1). The seismogenic zones of the FRI zonation (Slejko et al. 2008) have been added to the linear sources, in order to consider minor seismicity, which has been interpolated with the GR model after having removed the strong earthquakes already associated with the faults.

As an oil pipeline is an important structure, critical from the point of view of the seismic risk associated with damage to its various elements (tank, pipeline, pumping stations), it has been also decided to use as seismic sources, in addition to those of DISS, some

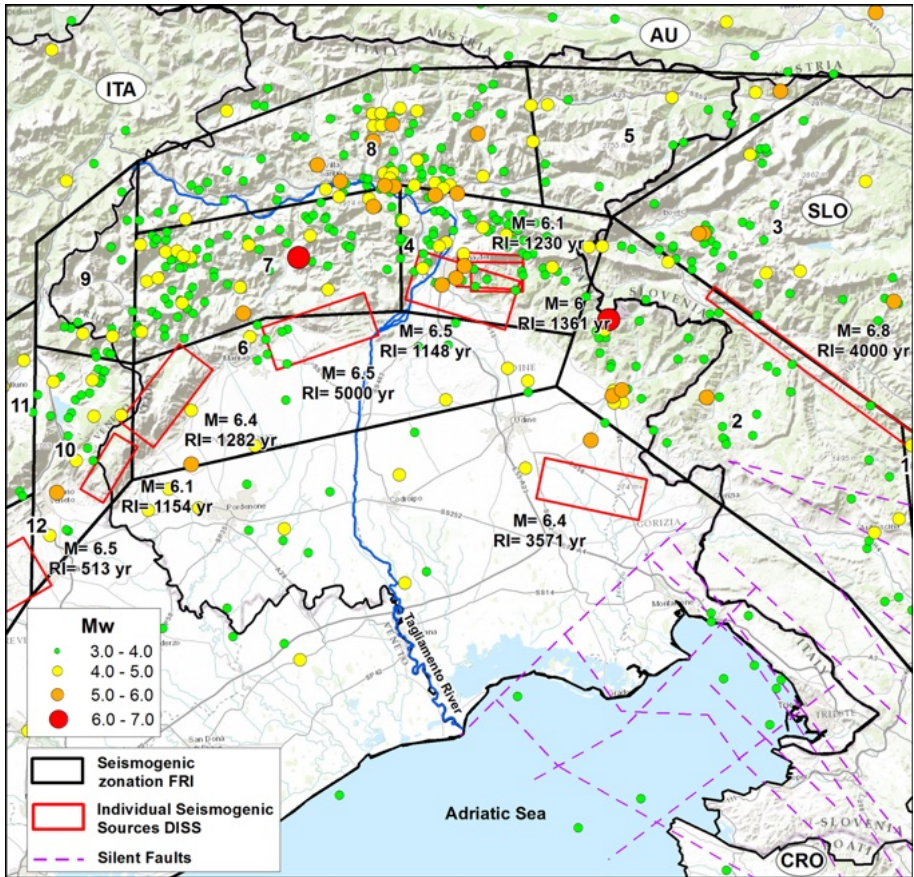


**Fig. 2** Seismic sources used for PSHA: FRI seismogenic zones (black boxes) and DISS faults (red boxes). The “silent faults” considered in the hazard computation are shown as well (purple dashed lines), together with the epicentres of earthquakes. In the seismogenic zones with DISS sources, only earthquakes with a magnitude lower than 6.0 are shown

Quaternary faults without documented seismicity but long enough to justify, at least, a characteristic magnitude of 6. These faults are located in the broader area of the Trieste Gulf and have been defined “silent faults” (Slejko et al. 2011a). Since it is impossible to evaluate the recurrence interval (RI) of these “silent faults” (the largest recorded earthquake occurred offshore of Punta Salvo in 1931 with a magnitude of 4.6), Slejko et al. (2011a) proposed a 10,000-year RI for the thrust faults and a 5000-year RI for the strike-slip faults, as the latter faults cut the former ones (see Table 2).

Seismic hazard in Friuli Venezia Giulia in terms of PGA and PGV with a 2475-year  $T_r$  for three soil types (rock, stiff and soft) is reported in Fig. 3. The results show that the strongest ground motions are expected in central Friuli, with values ranging from 0.6 to 1.2 g, and 45 to 65 cm/s, respectively for PGA and PGV (Fig. 3b, d), according to the soil type (the average regional increment for stiff and soft soils with respect to rock are 1.4 and 1.7, respectively, in the case of PGA, and 1.6 and 1.9 in the case of PGV); there, the presence of three individual sources with long RIs contribute notably. An additional

**Table 1** List of individual seismic sources reported in DISS (DISS Working Group 2010) used in this work, and their main characteristics

Code	Name	Length (km)	Width (km)	Min h (km)	Max h (km)	RI (years)	Eq	Max $M_w$
ITIS101	Montello	22	11.2	1.0	8.2	513	Unknown	6.5 <sup>a</sup>
ITIS102	Bassano-Cornuda	18	9.5	1.0	6.4	1724	25/02/1695	6.6 <sup>b</sup>
ITIS108	Maniago	8	5.5	0.5	3.3	1941	10/07/1776	5.9 <sup>b</sup>
ITIS109	Sequals	16.5	9.0	1.0	6.8	5000	Unknown	6.5 <sup>a</sup>
ITIS112	Tramonti	6	4.5	1.0	3.6	660	07/06/1794	5.8 <sup>b</sup>
ITIS113	Monte Grappa	5	3.9	0.5	2.7	400	12/06/1836	5.5 <sup>b</sup>
ITIS119	Tarcento	6	4.5	2.0	4.3	793	11/09/1976	5.7 <sup>b</sup>
ITIS120	Gemona South	16	9.0	2.0	6.5	1148	06/05/1976	6.5 <sup>b</sup>
ITIS121	Montenars	8	5.5	2.0	5.2	1361	15/09/1976	6.0 <sup>b</sup>
ITIS122	Gemona East	10	6.4	6.5	10.2	1230	15/09/1976	6.1 <sup>b</sup>
ITIS124	Cansiglio	10	6.4	1.5	6.4	1154	18/10/1936	6.1 <sup>b</sup>
ITIS125	Polcenigo-Montereale	15	8.5	2.0	7.5	1282	29/06/1873	6.4 <sup>b</sup>
ITIS126	Medea	16	9.0	0.5	6.9	3571	Unknown	6.4 <sup>a</sup>
ITIS127	Thiene-Bassano	18	9.5	1.0	5.8	1500	Unknown	6.6 <sup>a</sup>
SIIS001	Idrija	50	12.6	1.0	13.4	2000	26/03/1511	6.8 <sup>c</sup>
SIIS002	Bovec-Krn	13	6.3	3.0	9.2	360	12/04/1998	5.7 <sup>d</sup>

*Name* seismic source name, *h* depth, *RI* recurrence interval, *Eq* date of the latest earthquake  $M_w$  moment magnitude

<sup>a</sup>Calculated using the Wells and Coppersmith (1994) relationships

<sup>b</sup>Value adopted from the historical earthquake catalogue CPTI04

<sup>c</sup>Value adopted from Fitzko et al. (2005)

<sup>d</sup>Based on seismological data

computation has been performed for the 475-year  $T_r$  in order to establish a comparison of the present results with those of the Italian seismic code (NTC 2008) for ordinary buildings. In this case, the strongest ground shakings are expected in the western sector of central Friuli, with values ranging from 0.3 to 0.7 g, according to the soil type, and 25 to 45 cm/s, respectively for PGA and PGV (Fig. 3a, c).

The official Italian seismic hazard map (Stucchi et al. 2011), referring to a 475-year  $T_r$  and rock soil, identifies an E–W oriented strip with expected PGA of 0.250–0.275 g in central Friuli, conversely, in Fig. 3a (left panel) a PGA of 0.3–0.4 g pertains to central Friuli and the area with a PGA of 0.2–0.3 g covers the whole central-northern sector of the



**Table 2** List of the “silent faults” (Slejko et al. 2011a) used in this work, and their main characteristics

Cod.	Fault name	Type	Length (km)	M <sub>w</sub>	RI (years)
2	Aquileia	Strike-slip	50	6.5	5000
3a	Grado–Buzet offshore NW	Reverse	15	6.1	10,000
3b	Grado–Buzet offshore SE	Reverse	20	6.2	10,000
3c	Grado–Buzet NW	Reverse	18	6.2	10,000
3d	Grado–Buzet SE	Reverse	15	6.1	10,000
4	Sistiana	Strike-slip	44	6.5	5000
5	Mt. Spaccato	Strike-slip	51	6.5	5000
6a	Buje offshore NW	Reverse	17	6.1	10,000
6b	Buje offshore SE	Reverse	15	6.1	10,000
6c	Buje SE	Reverse	38	6.3	10,000
7a	Tinjan offshore	Reverse	13	6.0	10,000
7b	Tinjan	Reverse	15	6.1	10,000
8a	Palmanova NW	Reverse	17	6.1	10,000
8b	Palmanova centre	Reverse	18	6.2	10,000
8c	Palmanova S	Reverse	57	6.6	10,000
9a	Trieste NW	Reverse	17	6.1	10,000
9b	Trieste centre	Reverse	19	6.2	10,000
9c	Trieste SE	Reverse	36	6.3	10,000
10	Divaca	Strike-slip	50	6.5	10,000
11	Rasa	Strike-slip	30	6.3	10,000
12	Sneznik	Reverse	61	6.6	5556
13	Nanos R 33	Reverse	33	6.3	10,000
14	Trnovski Go	Reverse	37	6.3	10,000

region. This increase of expected ground shaking is motivated by the more articulated seismogenic zonation used in the present study and the different GMPE considered.

As the seismic behaviour of underground pipes is strongly influenced by the local soil conditions, we have combined the hazard results of the three soil types in a single map (*soil seismic hazard map*), on the basis of the lithological characterization proposed by Carulli (2006a, b) and through GIS technology. Figure 4 shows the method used to create a soil seismic hazard map. A soil map was used as input (Fig. 4a), and within it, the territory was differentiated into the three categories of the Italian seismic code (NTC 2008): rock, stiff soil, and soft soil. The hazard maps (Fig. 4b) computed for the different soil types, have, then, been intersected with the soil map using the spatial analysis of the GIS, obtaining the hazard extractions for each soil type in their actual position. Finally, the three maps were combined through a mosaic operation into the final soil seismic hazard map (Fig. 4c). The PGA and PGV maps (Fig. 5) show that the seismic hazard is considerably higher in the Alpine (northern mountain part of the region) valleys and on the Friuli Plain (southern part of the region) than in the mountain sector. The highest values can be seen in the morainic amphitheatre of the River Tagliamento Straits, in central Friuli, with values exceeding 1 g and 60 cm/s, for PGA and PGV, respectively.

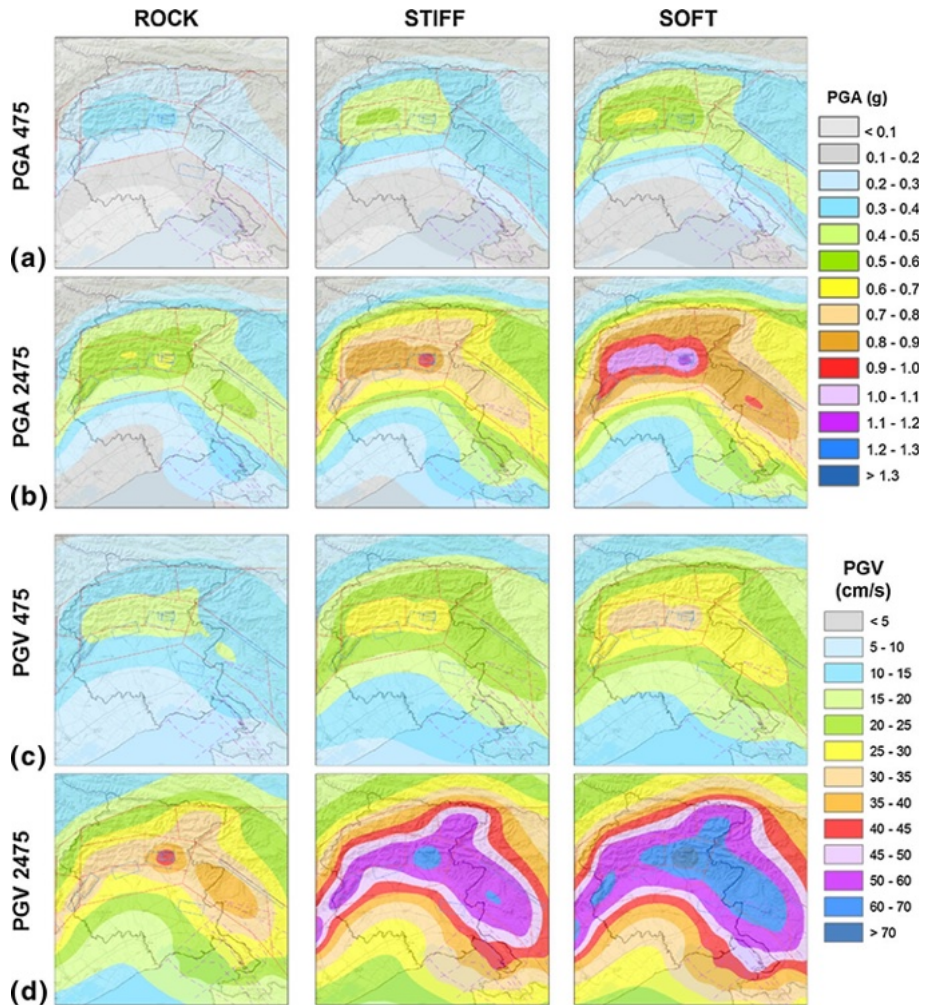


**Fig. 3** Seismic hazard in Friuli-Venezia Giulia for three soil types (rock, stiff, soft soil): **a** PGA with a 475-year Tr; **b** PGA with a 2475-year Tr; **c** PGV with a 475-year Tr; **d** PGV with a 2475-year Tr

The ground motion associated with each of the elements of the oil pipeline can be found in Table 3, where the great impact of the soil type on the results is highlighted: the Trieste Marine Terminal and Tank Farm are only 5 km distant but are built on different soils: the former on soft soil and the latter on rock. This situation implies a remarkable increase, both of PGA and PGV, in the Marine Terminal site with respect to those at the Tank Park site. Considering the absolute values, the pumping station C2, placed near Cavazzo Lake, ends up being the site with the highest seismic hazard, with PGA and PGV values respectively of 0.80 g and 52 cm/s.

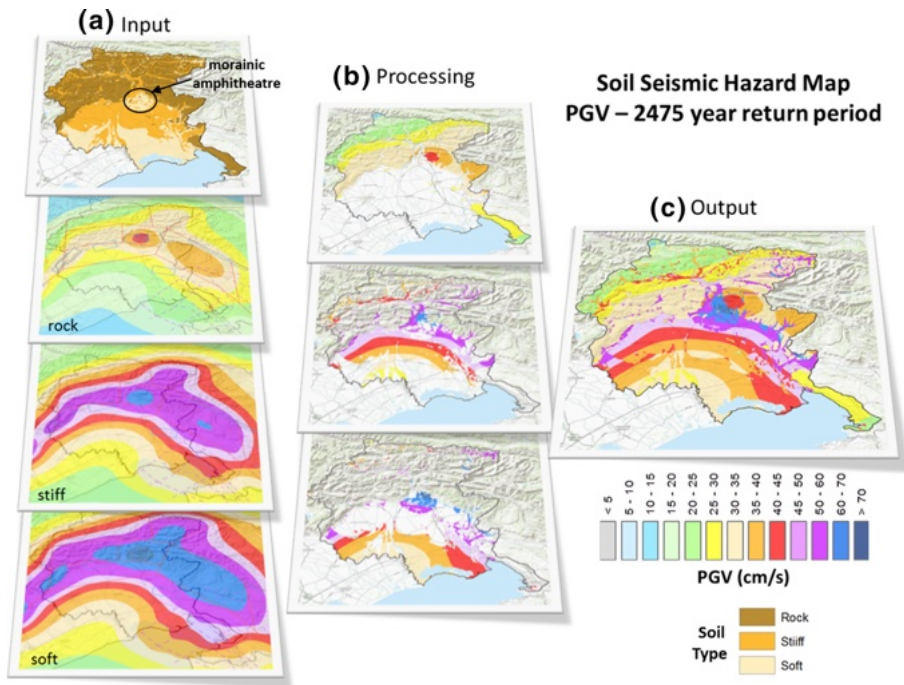


**Fig. 4** Scheme for the construction of the soil seismic hazard maps. The soil map has been used as input (top of panel **a**), with the territory differentiated into the three soil categories of the Italian seismic code (NTC 2008): rock, stiff, and soft. The hazard maps computed for the different soil types (lower part of panel **a**) have, then, been intersected with the soil map, using the spatial analysis of the GIS, and obtaining the aerial extraction of the expected ground motion for each soil type (**b**) in its actual position. Finally, the three maps were aggregated through a mosaic operation in the final soil seismic hazard map (**c**)

#### 4 Oil pipeline system vulnerability

The seismic risk in this case study is expressed in terms of direct physical damage, evaluated through empirically calculated fragility curves (see Fig. 6). The application of these curves requires the following data: the element classification (e.g., pipeline, oil storage tank, etc.), the definition of the expected damage levels (e.g., small, low, high), and the ground motion values (e.g., PGA, PGV). The ground motion values are associated with the studied element and represent the random variable that is modelled by a log-normal distribution. Finally, further data are the average value and the standard deviation of the fragility curves that change in function of the element type and the estimated damage level.

On the basis of the America Lifeline Alliance guidelines (ALA 2001), the seismic vulnerability of the underground structure is described by curves that associate the ground motion (PGA or PGV) to a performance indicator, such as the “Repair Rate”, that is the ratio between the number of repairs and the length of the pipeline (in km). This performance indicator was estimated from empirical (observational) data.

In the present study, the Lanzano et al. (2013a, b) methodology has been applied: it considers the consequences (e.g., the environmental pollution) caused by the damage suffered by the infrastructure. More precisely, Lanzano et al. (2013a, b) proposed for pipes a classification the state of risk (SR: representing, e.g., the negative effects of loss of

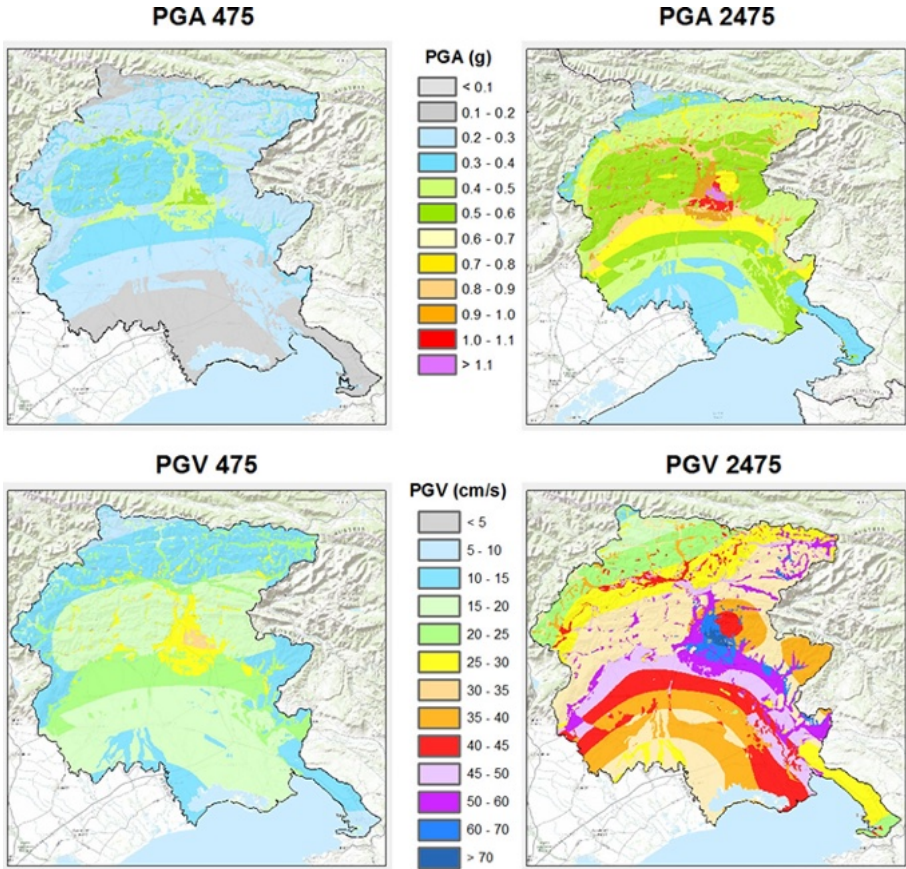


**Fig. 5** Soil seismic hazard maps. Both the PGA and PGV maps show a considerably higher seismic hazard in the Alpine valleys and, at a lesser extent, in the Friuli Plain than in the mountain sectors. The highest values are found in the morainic amphitheatre along the River Tagliamento, in central Friuli

**Table 3** PGA (g) and PGV (cm/s) for the five elements taken into consideration in this study

Element typology	Soil type	Tr = 475		Tr = 2475	
		PGA (g)	PGV (cm/s)	PGA (g)	PGV (cm/s)
Station C1	Stiff	0.35	19	0.61	35
Station C2	Stiff	0.46	26	0.80	52
Station C3	Stiff	0.35	23	0.69	51
Marine terminal	Soft	0.20	17	0.58	46
Tank farm	Rock	0.12	9	0.31	23

containment: see Table 4). These fragility curves were empirically defined and quantify the probability to reach a certain state of risk as function of the chosen shaking parameter (e.g., PGA or PGV).

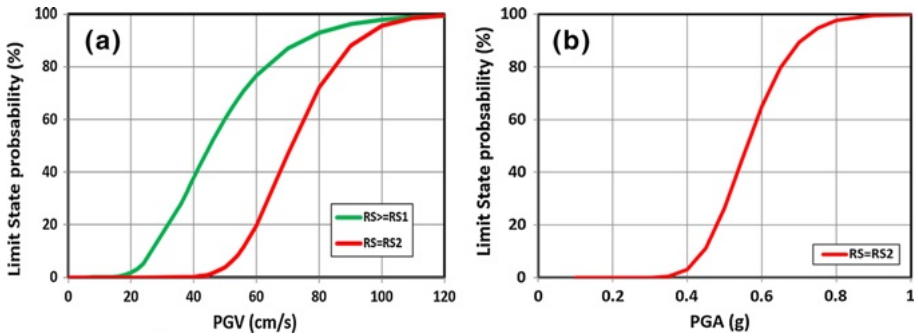


**Fig. 6** Fragility curves for a continuous pipeline interested by: **a** transient deformation (Lanzano et al. 2013a); **b** permanent deformation (Lanzano et al. 2013b). The RS description is given in Table 4

**Table 4** States of risk for pipes (Lanzano et al. 2013a)

RS	Level	Release of oil
RS0	Null	No loss of fluid
RS1	Low	Limited and time-distributed loss of fluid
RS2	High	Extensive or multiple losses

The Lanzano et al. (2013a) methodology considers two types of vulnerability for underground pipes: the first in the case of pipes submitted to transient deformations induced by shear waves (Lanzano et al. 2013a), and the second in the case of permanent ground deformations (Lanzano et al. 2013b). In the first case, PGV is the ground motion parameter related to risk, according to the Newmark (1967) simplified model, while PGA is the correlated parameter for the permanent ground deformations. Lanzano et al. (2013b) justified the choice of this seismic parameter because of the frequent use of scaling laws relating PGA, easily obtained through GMPEs, to permanent ground displacement (PGD) along the fault (represented by lateral spreading, seismic subsidence or induced by landslides). The structural elements have been classified according to the HAZUS methodology (FEMA 1999) and assume ductile continuum pipes (CP) in steel and with flanged joints, used for oil transportation. The fragility curves of Lanzano et al. (2013a, b) for a continuous pipeline are shown in Fig. 6: the curves represent, respectively, the probability for a continuous pipeline to reach certain risk states as function of PGV (Fig. 6a) and the probability to be interested by ground failure as function of PGA (Fig. 6b).

For the oil storage plant, the evaluation of damage caused by ground shaking, and the consequent toxic leakage, has been based on fragility curves (Fig. 7c) calibrated on empirical (observational) data by Fabbrocino et al. (2005) whose risk states (Table 5) have been taken into account together with the coefficients of the fragility curves for nearly full, as well as more than 50% full, anchored atmospheric steel tanks.

In addition to the oil storage tank and the pipeline that transports crude oil, the TAL oil transportation system consists of three pumping stations, which can also suffer damage caused by earthquakes. In the literature, there are several fragility curves as a function of PGA (Fig. 8c), and only a few as a function of PGD (not considered in present study) in the case of stations located in areas vulnerable to liquefaction or exposed to landslide

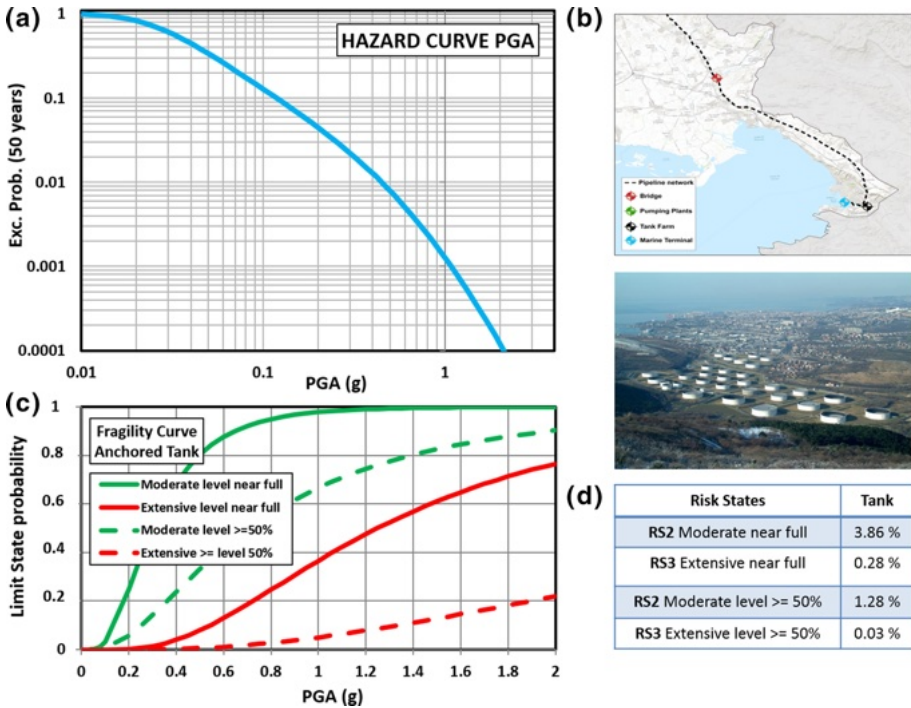


**Fig. 7** Expected damage to the TAL oil storage tank: **a** hazard curve; **b** station location; **c** fragility curves (Fabbrocino et al. 2005); **d** expected loss of containment

**Table 5** States of risk for oil storages (Fabbrocino et al. 2005)

RS	Level	Content losses
RS1	Null	No loss
RS2	Low	Moderate loss of containment
RS3	High	Extensive loss of containment

phenomena. For our case study, the damage states for these components have been associated with PGA, according to the four levels described in Table 6 (NIBS 2004).

### 5 Expected loss of containment of the oil system

Figure 7 shows the expected loss of containment calculated for the anchored atmospheric steel tanks (see their location in Fig. 7b). The hazard curves (Fig. 7a) calculated for the site where the storage tanks are located have been linked to fragility curves (Fig. 7c), considering the two risk states (moderate and extensive) considered by Fabbrocino et al. (2005) and for two different levels of oil, e.g., near full and filled more than 50%. The table in Fig. 7d shows the computed risk values in terms of probability of loss of containment: a maximum value of about 4% refers to the case of loss of containment for a nearly full tank.

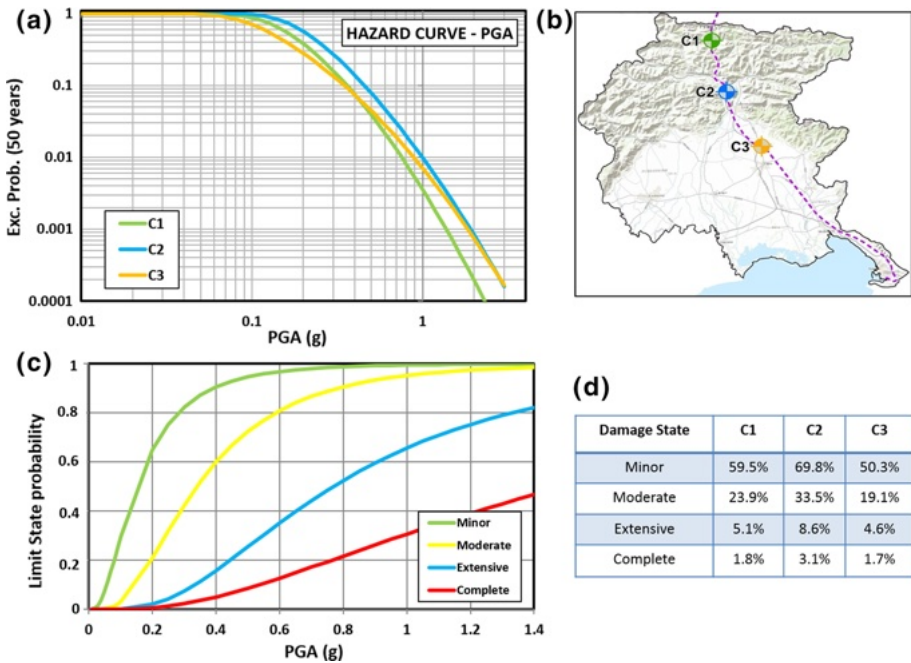


**Fig. 8** Expected damage to TAL pumping stations: **a** hazard curves; **b** station locations; **c** fragility curves (NIBS 2004); **d** expected damage

**Table 6** Damage state for pumping stations suggested by the HAZUS methodology (NIBS 2004)

DS	Level	Structural damage
DS1	Null	No damage
DS2	Minor	Small structure damage
DS3	Moderate	Significant damage to mechanical and electrical equipment and to the hosting facility
DS4	Extensive	Highly damaged structure and electric pumps
DS5	Complete	Structure collapse

Figure 8 shows the expected damage calculated for the three pumping stations C1, C2, C3 (see their location in Fig. 8b). The hazard curves (Fig. 8a) calculated for the sites where the stations are located have been linked to fragility curves (Fig. 8c) for the four damage states (see Table 6). The table in Fig. 8d shows the computed risk values, in terms of damage probability in 50 years: the pumping station C2 proves to be the most vulnerable, with almost 70% probability for minor, 33% for moderate, more than 8% for extensive, and a little more than 3% for complete damage.

Figures 9 and 10 show the seismic risk of the pipeline, in terms of probability in 50 years for the two risk states of loss of containment (Table 4) in external environment obtained through the convolution between the hazard curve (using PGV as shaking parameter), computed with a regular sampling along the oil pipeline route (not shown), and

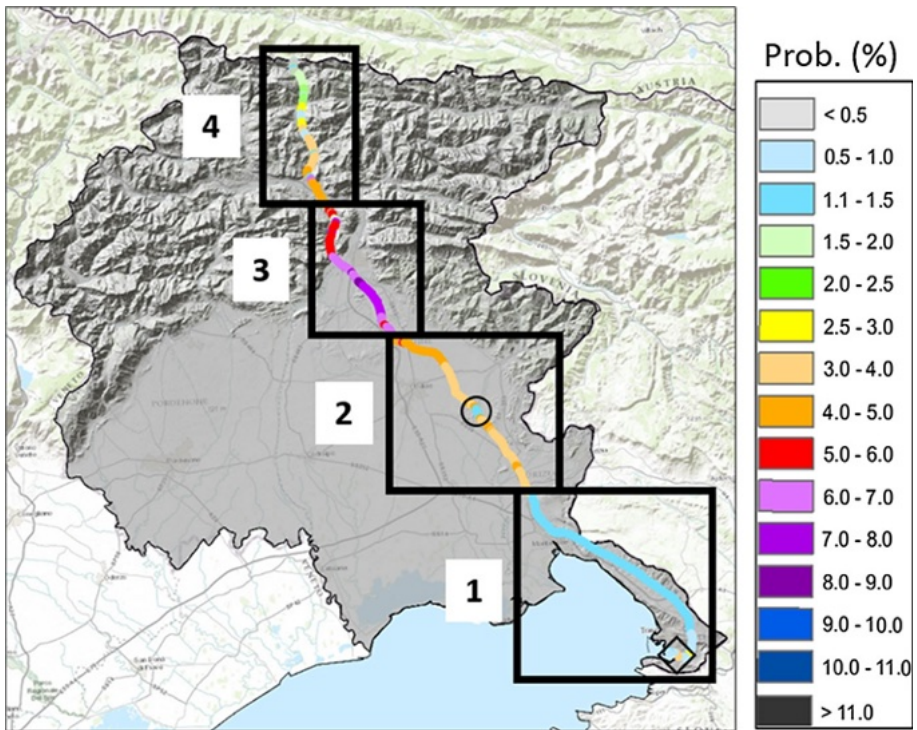


**Fig. 9** Probability in 50 years for a low risk state of content loss from the oil pipeline in the external environment caused by a transient deformation. The black circle identifies the segment of the pipeline where a high risk has been estimated in area 1, the diamond where a low risk has been computed in area 2

the fragility curves (Fig. 6a) of Lanzano et al. (2013a), in the case that the pipeline is submitted to transient deformations. Entering into details, Fig. 9 shows the results obtained for the low risk state, in which a limited loss of containment could happen.

Based on the obtained results, the pipeline route has been divided into four areas with different content loss percentages:

- *Area 1* in this area, a very low probability (between 0.5 and 3.5%) of content loss has been obtained, motivated by the low values of PGV. The segment of oil pipeline in the black diamond, where a probability of 3.5% is reached, is characterized by the fact that the pipeline, in that area, crosses soft soils characterized by the related amplification with respect to rocky sites;
- *Area 2* in this area, slightly higher risk has been obtained compared to the previous area, with a probability of content loss between 3 and 5%. The pipeline segment with a 1–1.5% probability is located at the east side of the rocky Buttrio hill (black circle), according to the litoseismic classification of Carulli (2006a, b), where a lower PGV is expected with respect to the surrounding (stiff and soft) soils;
- *Area 3* in this area, the highest risk along the whole pipeline route has been obtained, with a probability of content loss between 5 and 8.1%. This value is motivated by the high PGV produced in the hazard calculation by the presence in a few kilometres from the pipeline route of three individual DISS sources (see Fig. 2) with maximum magnitude higher than 6;



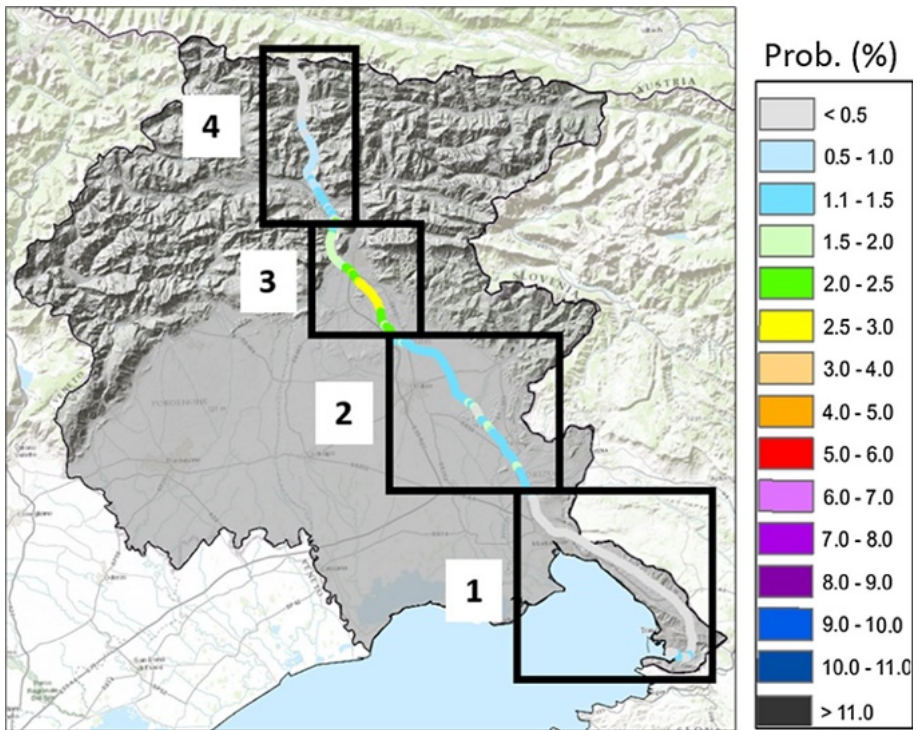


**Fig. 10** Probability in 50 years for a high risk state of content loss from the oil pipeline in the external environment caused by a transient deformations

- *Area 4* in this area, a probability of about 4% of content loss has been obtained in the southernmost segment of the pipeline; this percentage decreases (lower than 0.5%) moving northwards.

Figure 10 shows the results obtained for the high risk state (Table 5), that considers an extensive content loss. Also in this case, a subdivision of the whole pipe route into four segments is proposed, on the basis of the results obtained. For each of the four segments, a 35–40% decrease of probability of content loss has been obtained with respect to the low risk state (Fig. 9). For example, in the area 3, where the highest (8.1%) probability of content loss has been calculated for the low risk state (Fig. 9), only a 2.8% probability of content loss has been computed for the high risk state (Fig. 10).

Figure 11 represent the probability of content loss of dangerous substances in 50 years, in the case that the pipeline is submitted to permanent deformations. The Lanzano et al. (2013b) fragility curve, shown in Fig. 6b, is defined in this case, considering PGA as seismic parameter. In agreement with the previous considerations, also in this case the pipeline route has been divided into four segments, where a different loss of contaminant substances is expected:

- *Area 1* with a very low probability (lower than 1.5%) of content loss;
- *Area 2* with a slightly higher probability (between 2.0 and 4.5%) of content loss;

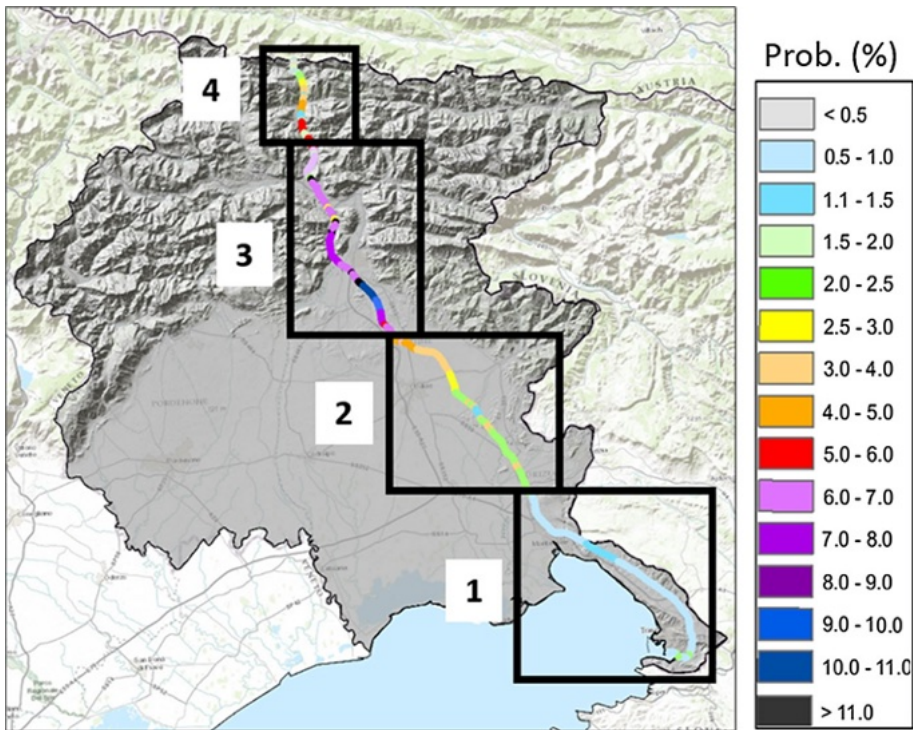


**Fig. 11** Probability in 50 years for the high risk state of content loss from the oil pipeline in the external environment caused by permanent deformations

- Area 3 with a higher probability (between 6 and 11.5%) of content loss; moreover it results of wider spatial extension compared to the previous cases of transient deformations (see Fig. 10).
- Area 4 with a low probability (lower than 6%) of content loss.

## 6 Final considerations

The soil hazard map has allowed us to characterize the expected ground motion, taking into account the local amplification determined by the specific geological features of the territory. In particular, the comparison of the results obtained for both PGA and PGV for the 2475-year Tr (Fig. 5) with the results obtained for a 475-year Tr illustrates the significant effect of three linear seismic sources located in central eastern Friuli, which have a RI longer than 1200 years.

The estimate of the content loss risk in the external environment (possible release of hazardous substances) for the TAL system in Friuli (NE Italy), based on fragility curves and taking into account the consequences of a possible pipe rupture (Table 4), is characterized by very low probability values with regard to a transient deformation (Figs. 9, 10), while the probability is slightly higher in the case of permanent deformation (Fig. 11). It must be pointed out that the latter indication refers to the effect of ground motion only

(in terms of PGA) and does not consider induced phenomena such as soil liquefaction and landslides; this choice is motivated by the fact that the present risk analysis is performed at a regional scale and, therefore, the use of the fragility curves developed by Lanzano et al. (2013b) seem to be suitable for a preliminary individuation of the areas along the pipeline route characterized by the major risk of content loss when the pipeline is subjected to a strong ground shaking.

The division of the pipeline route into four segments with a different risk of content loss of contaminant substances allow us to identify the places with major criticality (larger probability of loss in external environment) generated by strong ground motion along the TAL infrastructure route crossing the Friuli Venezia Giulia territory.

Regarding the steel tanks anchored, the probability of damage in 50 years, caused by the ground shaking, and the consequent loss of dangerous substances in the environment, have been computed by the convolution between the hazard curve related to the site and the fragility curves of Fabbrocino et al. (2005): using those fragility curves a lower (about 1/3) risk has been obtained in the case of a 50% full tank compared to an almost full tank (Fig. 7).

A rather high probability (almost 70% in 50 years) has been calculated for a minor damage in the case of the pumping station C2, located in central Friuli (Fig. 8), where the highest level of seismic hazard is expected (Fig. 5).

The results obtained in the present study, reported in Figs. 7, 8, 9, 10, and 11, represent a useful decision-making support for planning specific countermeasures and furnish an important information for emergency management. Moreover, the use of the GIS technology has been demonstrated to be very efficient for the analysis of seismic risk at a large scale, when a significant amount of data must be manipulated and processed. Therefore, the use of the GIS environment is a fundamental support tool for activities with the purpose of land-use planning and analysis of both structural and environmental risk mitigation.

## References

- ALA (American Lifeline Alliance) (2001) Seismic fragility formulations for water system. American Society of Civil Engineers (ASCE) and Federal Emergency Management Agency (FEMA)
- Bindi D, Pacor F, Luzi L, Puglia R, Massa M, Ameri G, Paolucci R (2011) Ground motion prediction equations derived from the Italian strong motion database. *Bull Earthq Eng* 9:1899–1920
- Bogliolo MP (2012) Proposal of a reference geo-database to support safety tasks involving the land context of Seveso establishments. *Chem Eng Trans* 26:483–488
- Campedel M, Cozzani V, Garcia-Agreda A, Salzano E (2008) Extending the quantitative assessment of industrial risks to earthquake effects. *Risk Anal* 28:1231–1246
- Carulli GB (2006a) Carta geologica del Friuli Venezia Giulia, scala 1:150.000, Regione Autonoma Friuli Venezia Giulia, Direzione Regionale Ambiente e Lavori Pubblici, Servizio Geologico Regionale
- Carulli GB (2006b) Note illustrative della Carta geologica del Friuli Venezia Giulia, scala 1:150.000, Regione Autonoma Friuli Venezia Giulia, Direzione Regionale Ambiente e Lavori Pubblici, Servizio Geologico Regionale, Selca, Firenze
- Clemente P (2013) Sicurezza sismica delle strutture industriali. Sicurezza sismica degli impianti chimici a rischio di incidente rilevante, pp 17–22
- Coppersmith KJ, Youngs RR (1986) Capturing uncertainty in probabilistic seismic hazard assessments within intraplate environments. In: Proceedings of the third U.S. national conference on earthquake engineering, August 24–28, 1986, Charleston, SC, Earthquake Engineering Research Institute, El Cerrito CA, USA, vol 1, pp 301–312
- Cornell CA (1968) Engineering seismic risk analysis. *Bull Seism Soc Am* 58:1583–1606

- DISS Working Group (2010) Database of Individual Seismogenic Sources (DISS), Version 3.1.1: a compilation of potential sources for earthquakes larger than M 5.5 in Italy and surrounding areas. Istituto Nazionale di Geofisica e Vulcanologia
- Eguchi RT (1983) Seismic vulnerability models for underground pipes. In: Proceedings of earthquake behavior and safety of oil and gas storage facilities, buried pipelines and equipment, ASME, PVP-77, New York, June, pp 368–373
- Fabbrocino G, Iervolino I, Orlando F, Salzano E (2005) Quantitative risk analysis of oil storage facilities in seismic areas. *J Hazard Mater* 123:61–69
- FEMA (1999) Earthquake loss estimation methodology HAZUS-MH. Technical manual, [www.fema.gov/hazus](http://www.fema.gov/hazus). Accessed 1/5/2012
- Fitzko FP, Suhadolc A, Aoudia, Panza GF (2005) Constraints on the location and mechanism of the 1511 Western-Slovenia earthquake from active tectonics and modeling of macroseismic data. *Tectonophysics* 404:77–90. <https://doi.org/10.1016/j.tecto.2005.05.003>
- Genn S (2014) Safety goals for seismic and tsunami risk: lessons learned from the Fukushima Daiichi disaster. *Nucl Eng Des* 280:449–463
- Girgin S (2011) The nanotech events during the 17 August 1999 Koaceli earthquake: aftermath and lessons learned. *Nat Hazards Earth Syst Sci* 11:1129–1140
- Grimaz S (2012) Fenomeni near-field come effetti di sito? Un'ipotesi di lavoro che trova riscontri anche nelle osservazioni sul campo in occasione dei recenti terremoti distruttivi italiani. In: Atti del 31° Convegno Nazionale Gruppo Nazionale di Geofisica della Terra Solida, Potenza, 20-22 novembre 2012
- Grimaz S (2014) Can earthquakes trigger serious industrial accidents in Italy? Some considerations following the experiences of 2009 L'Aquila (Italy) and 2012 Emilia (Italy) earthquakes. *Boll Geof Teor Appl* 55:227–237
- Grimaz S, Malisan P (2014) Near field domain effects and their consideration in the international and Italian seismic codes. *Boll Geof Teor Appl* 55(4):717–738
- Grimaz S, Slejko D (2014) Seismic hazard for critical facilities. *Boll Geof Teor Appl* 55:3–16
- Hamada M (1991) Estimation of earthquake damage to lifeline system in Japan. In: Proceeding of the third Japan-US workshop on earthquake resistant design of lifeline facilities and countermeasures for soil liquefaction, San Francisco, CA, December 17–19, 1990, Technical Report NCEER-91-0001, NCEER, State University of New York at Buffalo, Buffalo, NY, pp 5–22
- Isoyama R, Katayama T (1982) Reliability evaluation of water supply system during earthquakes. Report of the institute of Industrial science, University of Tokyo, vol 30
- Isoyama R, Ishida E, Yne K, Shirozu T (2000) Seismic damage estimation procedure for water supply pipelines. In: Twelfth world conference on earthquake engineering, paper no. 1762, 30 January–4 February, 2000, Auckland, New Zealand
- Katayama T, Kubo K, Sato N (1975) Earthquake damage to water and gas distribution systems. In: Proceedings of the U.S. national conference on earthquake engineering, EERI, Oakland, CA, pp 396–405
- Kijko A, Graham G (1998) Parametric-historic procedure for probabilistic seismic hazard analysis. Part I: estimation of maximum regional magnitude  $m_{max}$ . *Pure Appl Geophys* 152:413–442
- Krausmann E, Cozzani V, Salzano E, Renni E (2011) Industrial accidents triggered by natural hazards: an emerging risk issue. *Nat Hazards Earth Syst Sci* 11:921–929
- Kulkarni RB, Youngs RR, Coppersmith KJ (1984) Assessment of confidence intervals for results of seismic hazard analysis. In: Proceedings of the eighth world conference on earthquake engineering, July 21–28, 1984, San Francisco CA USA, vol 1. Prentice-Hall Inc., Englewood Cliffs, pp 263–270
- Lanzano G, Salzano E, Santucci, De Magistris F, Fabbrocino G (2013a) Performance assessment of continuous buried pipelines under earthquake loadings. *Chem Eng Trans* 31:631–636
- Lanzano G, Salzano E, De Magistris FS, Fabbrocino G (2013b) Vulnerability of pipelines subjected to permanent deformation due to geotechnical co-seismic effects. *Chem Eng Trans* 32:415–420
- Lindell MK, Perry RW (1997) Hazardous materials releases in the northridge earthquake: implications for seismic risk assessment. *Risk Anal* 17:147–156
- McGuire RK (1977) Seismic design spectra and mapping procedures using hazard analysis based directly on oscillator response. *Earthq Eng Struct Dyn* 5:211–234
- McGuire RK, Shedlock KM (1981) Statistical uncertainties in seismic hazard evaluations in the United States. *Bull Seism Soc Am* 71:1287–1308
- Newmark NM (1967) Problems in wave propagation in soil and rocks. In: Proceedings of the international symposium on wave propagation and dynamic properties of earth materials, University of New Mexico Press, pp 7–26
- NIBS (2004) Earthquake loss estimation methodology HAZUS. National Institute of Building Sciences, FEMA, Washington

- Norme Tecniche per le Costruzioni; 2008 D.M., 14 Jan 2008
- O'Rourke MJ, Ayala G (1993) Pipeline damage due to wave propagation. *J Geotech Eng ASCE* 119(9):1490–1498
- O'Rourke MJ, Liu X (1999) Response of buried pipelines subjected to earthquake effects. MCEER monograph no. 3, University of New York, Buffalo, USA
- O'Rourke TD, Stewart HE, Gowdy TE, Pease JW (1991) Lifeline and geotechnical aspect of the 1989 Loma Prieta earthquake. In: Proceedings of the second international conference on recent advances in geotechnical earthquake engineering and soil dynamics, St. Louis, MO, pp 1601–1612
- O'Rourke TD, Toprak S, Sano Y (1998) Factors affecting water supply damage caused by the Northridge earthquake. In: Proceedings of the sixth US national conference on earthquake engineering
- Ordaz M, Aguilar A, Arboleda J (2015) CRISIS2015, Ver. 2.0. Program for computing seismic hazard, UNAM, México
- Rebez A, Slejko D (2004) Introducing epistemic uncertainties into seismic hazard assessment for the broader Vittorio Veneto area (N.E. Italy). *Boll Geof Teor Appl* 45:305–320
- Schwartz DP, Coppersmith KJ (1984) Fault behaviour and characteristic earthquakes: examples from Wasatch and San Andreas faults. *J Geophys Res* 89:5681–5698
- Slejko D, Peruzza L, Rebez A (1998) Seismic hazard maps of Italy. *Ann Geofis* 41:183–214
- Slejko D, Rebez A, Santulin M (2008) Seismic hazard estimates for the Vittorio Veneto broader area (NE Italy). *Boll Geof Teor Appl* 49:329–356
- Slejko D, Carulli GB, Ruscetti M, Cucchi F, Grimaz S, Rebez A, Accaino F, Affatato A, Biolchi S, Nieto D, Puntel E, Sanò T, Santulin M, Tinivella U, Zini L (2011a) Soil characterization and seismic hazard maps for the Friuli Venezia Giulia region (NE Italy). *Boll Geof Teor Appl* 52:59–104
- Slejko D, Carulli GB, Garcia J, Santulin M (2011b) The contribution of “silent” faults to the seismic hazard of the northern Adriatic Sea. *J Geodyn* 51:166–178
- Stucchi M, Meletti C, Montaldo V, Crowley H, Calvi GM, Boschi E (2011) Seismic hazard assessment (2003–2009) for the Italian building code. *Bull Seism Soc Am* 101:1885–1911. <https://doi.org/10.1785/0120100130>
- Toro GR, Abrahamson NA, Schneider JF (1997) Model of strong motions from earthquakes in central and eastern North America: best estimates and uncertainties. *Seism Res Lett* 68:41–57
- Wells DL, Coppersmith KJ (1994) New empirical relationship among magnitude, rupture length, rupture width, rupture area, and surface displacement. *Bull Seism Soc Am* 84:974–1002